Available online at www.sciencedirect.com
ScienceDirect
Tetrahedron
Tetrahedron 63 (2007) 2875–2881

[3]Pseudorotaxanes based on the cryptand/monopyridinium salt recognition motif

Feihe Huang,[a,b,*] Carla Slebodnick,[b] Eric J. Mahan[b,†] and Harry W. Gibson[b,*]

[a]*Department of Chemistry, Zhejiang University, Hangzhou 310027, PR China*
[b]*Department of Chemistry, Virginia Polytechnic Institute and State University, Blacksburg, VA 24061-0212, USA*

Received 6 September 2006; revised 16 January 2007; accepted 18 January 2007
Available online 20 January 2007

Abstract—The first cryptand/monopyridinium salt [3]pseudorotaxanes were prepared from two cryptand hosts and two bispyridinium guests as confirmed by proton NMR characterization, electrospray ionization mass spectrometry, and X-ray analysis. It was found that the two monopyridinium binding sites are independent of each other for the formation of one [3]pseudorotaxane.
© 2007 Elsevier Ltd. All rights reserved.

1. Introduction

The design and preparation of interlocked threaded structures, such as pseudorotaxanes, rotaxanes, catenanes, polypseudorotaxanes, polyrotaxanes, and polycatenanes, are hot topics in chemistry due to not only their topological importance but also their potential applications including molecular machines and drug delivery materials.[1] Since the bipyridinium dication paraquat (*N*,*N*′-dimethyl-4,4′-bipyridinium) was used as the guest with bis(*p*-phenylene)-34-crown-10 as the macrocyclic host to prepare a [2]pseudorotaxane by the Stoddart group about two decades ago,[2] paraquat derivatives have been one of the most widely used families of guests in the preparation of threaded structures.[1a] Their hosts include not only crown ethers[2,3] but also bis(*m*-phenylene)-32-crown-10-based cryptands,[4] dibenzo-24-crown-8-based cylindrical macrocycles,[5] and other hosts.[6] However, monopyridinium-based threaded structures have been rarely reported. The only example is the Beer systems[7] based on ion-pair recognition by ditopic hosts and bis(*m*-phenylene)-32-crown-10/monopyridinium and cryptand/monopyridinium [2]pseudorotaxanes we reported recently.[8] This is strange considering the wide use of monopyridinium salts in chemistry not only due to their easy availability but also because of their potential applications.[9] For the most recent examples, they have been used in the synthesis of novel monomeric and homodimeric cyanine dyes for nucleic acid detection,[9e] preparation of cationic lipids in gene delivery,[9f] fabrication of novel stilbazolium analogs as second-order nonlinear optical materials,[9g] and manufacture of amperometric sensors.[9h] Furthermore, the study of pseudorotaxanes based on the recognition of monopyridinium salt guests by macrocyclic hosts is very important, because the formation of these pseudorotaxanes makes it easy to prepare paraquat-based mechanically interlocked threaded structures from neutral bipyridines.[10]

The fabrication of high order assemblies containing more than two components remains a considerably challenging task for supramolecular chemists,[11] so we are interested in making high order monopyridinium-based pseudorotaxanes after we prepared the first monopyridinium-based [2]pseudorotaxanes.[8] Herein we report the construction of the first monopyridinium-based [3]pseudorotaxanes from cryptand hosts **1**[4a,e] and linear bispyridinium guests **2** (Fig. 1). Furthermore, because the study of the formation mechanism of [3]pseudorotaxanes should be helpful for future higher order monopyridinium-based threaded structures, we studied how the two monopyridinium moieties of guest **2** interact with each other during its complexation with host **1** by using the Scatchard plot method.[12]

2. Results and discussion

2.1. Synthesis of cryptand hosts and bispyridinium guests

The preparation of bis(*m*-phenylene)-32-crown-10-based cryptand hosts **1** followed previously reported procedures.[4a,e] Bispyridinium salts **2** were prepared by the reaction of

Keywords: Host–guest systems; Self-assembly; Pseudorotaxane; Cryptand; Pyridinium.
* Corresponding authors. Tel.: +86 571 8795 3189; fax: +86 571 8795 1895 (F.H.); tel.: +1 540 231 5902; fax: +1 540 231 8517 (H.W.G.); e-mail addresses: fhuang@zju.edu.cn; hwgibson@vt.edu
† Present address: Department of Chemistry, University of Hartford, West Hartford, CT 06117, USA.

0040–4020/$ - see front matter © 2007 Elsevier Ltd. All rights reserved.
doi:10.1016/j.tet.2007.01.029

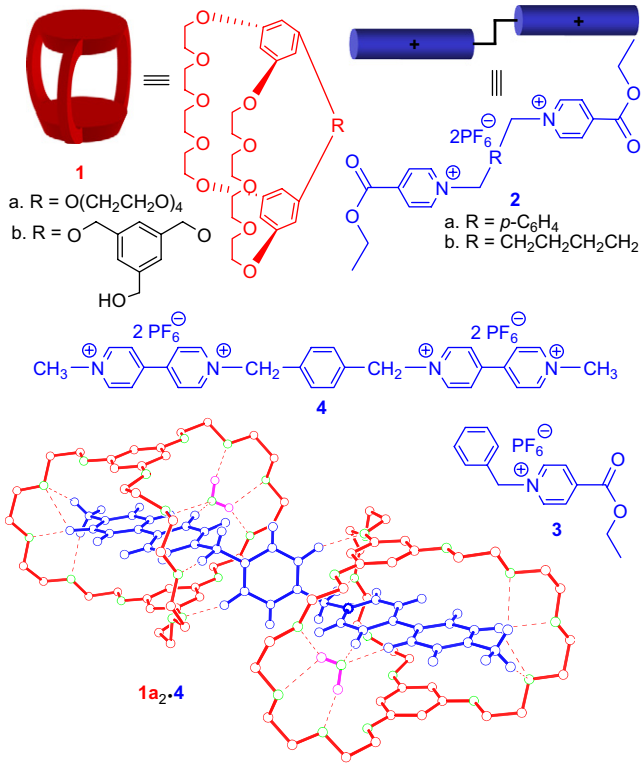

Figure 1. Compounds used in this study and the X-ray structure[4b] of $\mathbf{1a}_2\cdot\mathbf{4}$ with PF_6 counterions removed.

excess ethyl isonicotinate with 1,4-di(bromomethyl)benzene or 1,6-dibromohexane followed by ion exchange with ammonium hexafluorophosphate. They were purified by recrystallization in deionized water and dried under vacuum at 100 °C.

2.2. Proton NMR study

The yellow color of solutions of cryptand **1** and bispyridinium salts **2** is due to the charge transfer between the electron-rich phenylene rings of **1** and the electron-poor pyridinium rings of **2**. Partial proton NMR spectra of **1a**, **2a**, and a mixture of **1a** and **2a** are shown in Figure 2. Only one set of peaks was found in the proton NMR spectrum of the solution of **1a** and **2a**, indicating fast-exchange complexation. After complexation, peaks corresponding to β-pyridinium protons H_6 of **2a** and aromatic protons H_1 of **1a** moved upfield significantly. Furthermore, α-pyridinium protons H_7, phenylene protons H_9, and benzylic protons H_8, and ethyl ester methylene protons H_5 of **2a** and α- and β-ethyleneoxy protons (H_2 and H_4) of **1a** also moved upfield, while γ-ethyleneoxy protons H_3 of **1a** moved downfield. The stoichiometries of the complexes between cryptand **1** and bispyridinium salt **2** were determined to be 2:1 in solution by a mole ratio plot[13] using proton NMR data (Fig. 3).

2.3. Electrospray ionization mass spectrometry

Electrospray ionization mass spectra of solutions of **1a** and **2** in 4:1 acetonitrile–chloroform provided further support for the formation of 2:1 complexes between cryptand **1** and bispyridinium **2** in solution. For the mass spectrum of a solution of **1a** and **2a**, the base peak was at *m/z* 566.6, corresponding to $[\mathbf{1a}\cdot\mathbf{2a}-2PF_6]^{2+}$. One more peak was found for $\mathbf{1a}\cdot\mathbf{2a}$ at *m/z* 1277.6 (13%) $[\mathbf{1a}\cdot\mathbf{2a}-PF_6]^{+}$. Three peaks were found

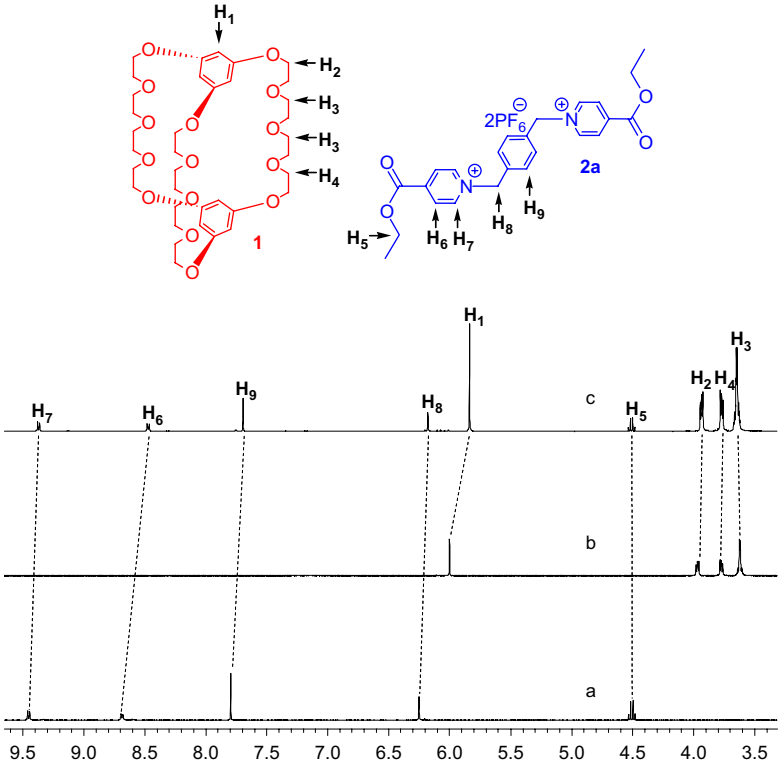

Figure 2. Partial proton NMR spectra (400 MHz, acetone-d_6, 22 °C) of bispyridinium salt **2a** (a, bottom), cryptand **1a** (b, middle), and 6.00 mM **1a** and 3.00 mM **2a** (c, top).

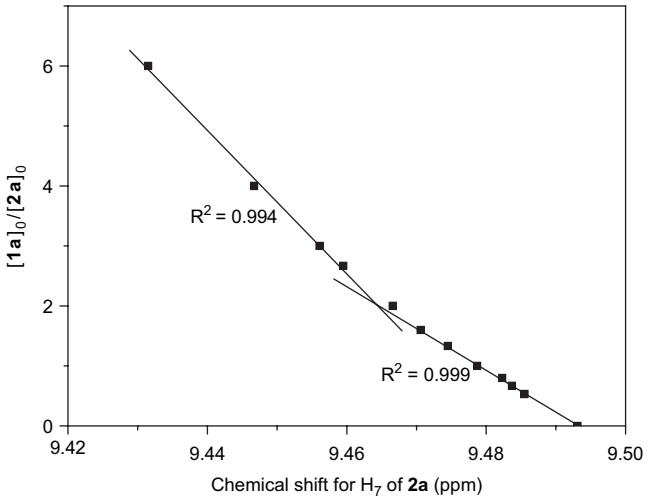

Figure 3. Mole ratio plot for **1a** and **2a**, indicating 2:1 stoichiometry. The solvent is acetone-d_6. $[\mathbf{2a}]_0$=0.250 mM.

for $\mathbf{1a}_2\cdot\mathbf{2a}$ at *m/z* 929.9 (19%) $[\mathbf{1a}_2\cdot\mathbf{2a}-2PF_6]^{2+}$, 915.7 (12%) $[\mathbf{1a}_2\cdot\mathbf{2a}-2PF_6-C_2H_4]^{2+}$, and 611.6 (6%) $[\mathbf{1a}_2\cdot\mathbf{2a}-2PF_6-C_2H_5OH+Na]^{3+}$. For the mass spectrum of a solution of **1a** and **2b**, the base peak was at *m/z* 556.6, corresponding to $[\mathbf{1a}\cdot\mathbf{2b}-2PF_6]^{2+}$. One more peak was found for $\mathbf{1a}\cdot\mathbf{2b}$ at *m/z* 1257.6 (15%) $[\mathbf{1a}\cdot\mathbf{2b}-PF_6]^{+}$. Two peaks were observed for $\mathbf{1a}_2\cdot\mathbf{2b}$ at *m/z* 919.8 (21%) $[\mathbf{1a}_2\cdot\mathbf{2b}-2PF_6]^{2+}$ and 601.5 (7%) $[\mathbf{1a}_2\cdot\mathbf{2a}-2PF_6-COOC_2H_5+K]^{3+}$.

2.4. Scatchard plot for complexation between bis(crown ether) host 1a and bispyridinium 2a

In order to study the relationship between the two monopyridinium binding sites of bispyridinium **2** during its complexation with cryptand **1**, we studied the complexation between **1a** and **2a** as an example by the Scatchard plot method. Proton NMR characterizations were done on a series of acetone solutions for which the initial concentration of guest **2a** was kept constant at 0.250 mM while the initial concentration of host **1a** was systematically varied. Based on these proton NMR data, the extent of complexation, *p*, of the monopyridinium units was determined[14] and a Scatchard plot[12] was drawn (Fig. 4). The linear nature of this plot demonstrated that the two pyridinium binding sites are independent of each other during the complexation,[15] that is, the complexation between **1a** and **2a** is statistical. From the intercept and the slope of the plot, the average association constant[16] (K_{av}) is 2.8 ($\pm$0.3)$\times10^2$ M^{-1} for the complexation between **1a** and **2a**. This average association constant is little higher than the association constant, 182 M^{-1}, for $\mathbf{1a}\cdot\mathbf{3}$ in acetone,[8b] presumably due to the greater acidity of the pyridinium hydrogens of **2a** than those of **3** because the phenylene ring was shared by two pyridinium rings in bispyridinium salt **2a** while it was shared by only one pyridinium ring in monopyridinium salt **3**.

2.5. X-ray analysis of [3]pseudorotaxane $\mathbf{1a}_2\cdot\mathbf{2a}$

Ultimate proof for the formation of [3]pseudorotaxanes $\mathbf{1}_2\cdot\mathbf{2}$ based on the cryptand/monopyridinium recognition motif is from X-ray analysis (Figs. 5–7).[17] X-ray quality, yellow single crystals of $\mathbf{1a}_2\cdot\mathbf{2a}$ were grown by vapor diffusion of pentane into an acetonitrile solution of **2a** with excess **1a**. As in the 1:1 complex between cryptand **1a** and **3**,[2] $\mathbf{1a}_2\cdot\mathbf{2a}$ is stabilized by hydrogen bonding and face-to-face π-stacking interactions (Fig. 5) and the ethyl ester methylene protons are involved in hydrogen bonding to ethyleneoxy oxygen atoms of cryptand **1a** (*A* and *B* of Fig. 5). An α-proton of each pyridinium unit is connected to an ethyleneoxy chain by a hydrogen-bonding water bridge (*C*–*E* of Fig. 5). The left α-pyridinium proton of each monopyridinium unit is directly hydrogen bonded to an ether oxygen (*F* of Fig. 5). Also as in $\mathbf{1a}\cdot\mathbf{3}$[8b] the distances between each pyridinium ring of **2a** and the phenylene rings of the cryptand host are about equal to each other, presumably in order to maximize face-to-face π-stacking between the electron-rich cryptand host and the electron-poor pyridinium moieties. However, there is still an obvious difference; that is, a benzylic proton is hydrogen bonded to an ethyleneoxy oxygen of the cryptand host **1a** in $\mathbf{1a}\cdot\mathbf{3}$,[8b] while none of the xylyl methylene protons are involved in hydrogen bonding in $\mathbf{1a}_2\cdot\mathbf{2a}$. The centroid–centroid distance between the phenylene rings of the cryptand host in $\mathbf{1a}_2\cdot\mathbf{2a}$ is 6.58 Å, while this distance

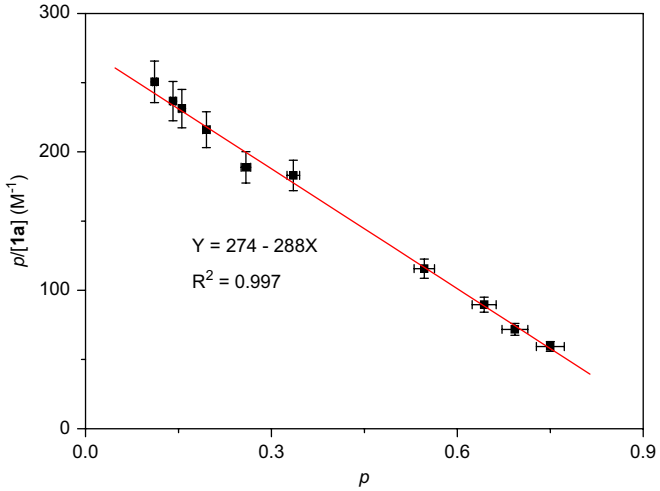

Figure 4. Scatchard plot for the complexation of cryptand host **1a** with bispyridinium guest **2a** in acetone-d_6 at 22 °C. *p*=fraction of monopyridinium units bound. Error bars in *p*: $\pm$0.03 absolute; error bars in *p*/[**1a**]: $\pm$0.06 relative.

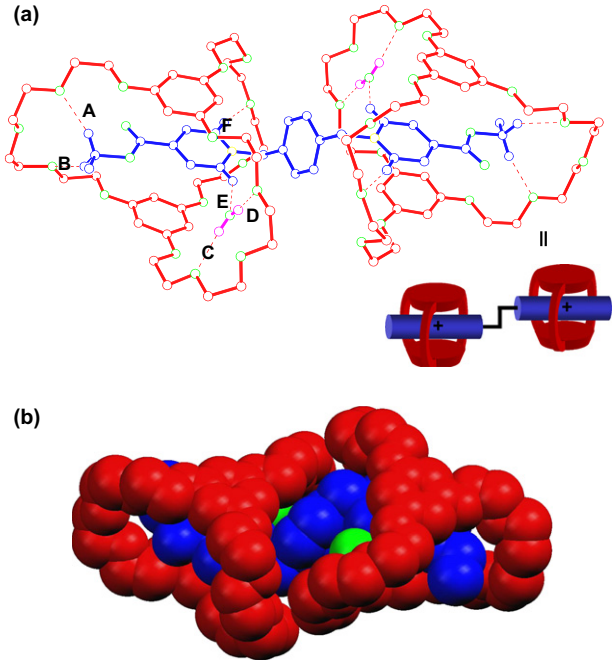

Figure 5. Ball-stick (a, top) and space-filling (b, bottom) views of the X-ray structure of $\mathbf{1a}_2\cdot\mathbf{2a}$. (a) Molecules **1a** are red, **2a** is blue, water molecules are magenta, oxygens are green, and nitrogens are yellow. Two PF_6 counterions, other solvent molecules, and the hydrogens except the ones involved in hydrogen bonding were omitted for clarity. Hydrogen-bond parameters: C(O)···O distances (Å), H···O distances (Å), C(O)–H···O angles (°) at *A*, 3.42, 2.53, 150; *B*, 3.21, 2.26, 161; *C*, 2.99, 2.15, 171; *D*, 2.92, 2.08, 173; *E*, 3.06, 2.28, 140; *F*, 3.41, 2.47, 170. Face-to-face π-stacking parameters: centroid–centroid distances (Å) 3.74, 3.66; ring plane/ring plane inclinations (°) 9.1, 4.8. (b) All protons, two PF_6 counterions, and other solvent molecules were omitted. Molecules **1a** are red, **2a** is blue, and the water molecules are green.

is 6.88 Å in $\mathbf{1a}\cdot\mathbf{3}$,[8b] indicating stronger charge transfer interactions between cryptand hosts and monopyridinium binding sites in $\mathbf{1a}_2\cdot\mathbf{2a}$ due to the increase of the positive charge density on the pyridinium rings of bispyridinium salt **2a** compared with that of monopyridinium salt **3**.[20] This result is in agreement with the higher average association constant for the complexation between cryptand **1a** and bispyridinium salt **2a** than between cryptand **1a** and monopyridinium salt **3**.

The ^{1}H NMR chemical shift changes of host **1a** upon complexation are consistent with a structure in solution similar to that of $\mathbf{1a}_2\cdot\mathbf{2a}$ in the solid state (Fig. 5). Protons H_1, H_2, and H_4 are in shielding regions of the aromatic guest, while H_3 resides in the deshielding environment of the central phenylene ring of the bispyridinium guest. The upfield shift of the ethyl ester methylene (H_5) and phenylene protons (H_9) of the guest **2a** is consistent with their positions in the shielding region of the aromatic moieties of the cryptand host **1a**.

Previously we reported a [3]pseudorotaxane $\mathbf{1a}_2\cdot\mathbf{4}$ from the cooperative complexation between cryptand host **1a** and bisparaquat guest **4**.[4b] Based on the X-ray structure of $\mathbf{1a}_2\cdot\mathbf{4}$ (Fig. 1), we claimed that one possible reason for this cooperative complexation was that the formation of the 1:1 complex effectively restricts rotation about the N–CH_2–C_6H_4 bonds of bisparaquat **4** because of the hydrogen bonding of both the xylyl methylene and *ortho* aromatic protons of

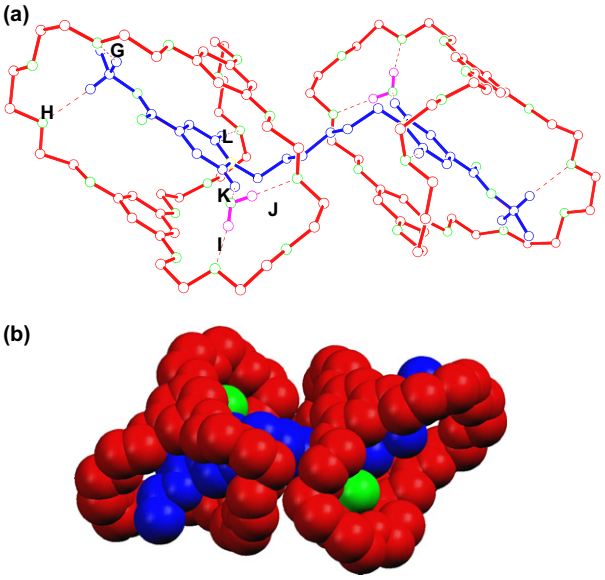

Figure 6. Ball-stick (a, top) and space-filling (b, bottom) views of the X-ray structure of $\mathbf{1a}_2\cdot\mathbf{2b}$. (a) Molecules **1a** are red, **2b** is blue, water molecules are magenta, oxygens are green, and nitrogens are yellow. Two PF_6 counterions, other solvent molecules, and the hydrogens except the ones involved in hydrogen bonding were omitted for clarity. Hydrogen-bond parameters: C(O)···O distances (Å), H···O distances (Å), C(O)–H···O angles (°) at *G*, 3.31, 2.45, 144; *H*, 3.34, 2.35, 171; *I*, 2.93, 1.97, 168; *J*, 2.85, 1.92, 167; *K*, 3.04, 2.32, 129; *L*, 3.25, 2.26, 173. Face-to-face π-stacking parameters: centroid–centroid distances (Å) 3.80, 3.74; ring plane/ring plane inclinations (°) 6.4, 5.4. (b) All protons, the PF_6 counterions, and other solvent molecules were omitted. Molecules **1a** are red, **2b** is blue, and the water molecules are green.

4 to cryptand host **1a** (see Fig. 1) and this conformational restriction facilitates complexation of the second paraquat site.[4b] Actually the observations here support this claim. From proton NMR characterization, we know that the

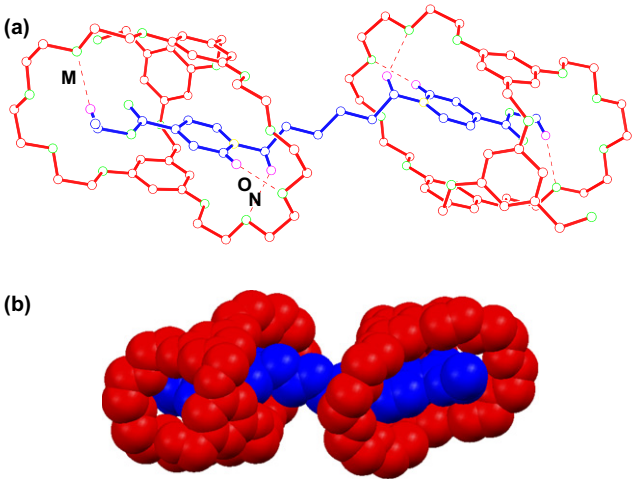

Figure 7. Ball-stick (a, top) and space-filling (b, bottom) views of the X-ray structure of $\mathbf{1b}_2\cdot\mathbf{2b}$. (a) Molecules **1b** are red, **2b** is blue, oxygens are green, and nitrogens are yellow. Two PF_6 counterions, solvent molecules, and the hydrogens except the ones involved in hydrogen bonding were omitted for clarity. Hydrogen-bond parameters: C···O distances (Å), H···O distances (Å), C–H···O angles (°) at *M*, 3.40, 2.52, 148; *N*, 3.37, 2.57, 138; *O*, 3.48, 2.56, 165. Face-to-face π-stacking parameters: centroid–centroid distances (Å) 4.03, 3.87; ring plane/ring plane inclinations (°) 7.5, 5.3. (b) All protons, the PF_6 counterions and solvent molecules were omitted. Molecules **1b** are red and **2b** is blue.

complexation between **1a** and **2a** is statistical. In the X-ray structure of $\mathbf{1a}_2\cdot\mathbf{2a}$, none of the xylyl methylene or central aromatic protons of **2a** are involved in hydrogen bonding to cryptand **1a** (Fig. 5).

Another difference between cryptand/bisparaquat [3]pseudorotaxane $\mathbf{1a}_2\cdot\mathbf{4}$ and cryptand/bispyridinium [3]pseudorotaxane $\mathbf{1a}_2\cdot\mathbf{2a}$ is that water molecules are hydrogen-bonding bridges between β-pyridinium protons of the guest and cryptand hosts in $\mathbf{1a}_2\cdot\mathbf{4}$, while they are hydrogen-bonding bridges between α-pyridinium protons and cryptand hosts in $\mathbf{1a}_2\cdot\mathbf{2a}$.

2.6. X-ray analysis of [3]pseudorotaxane $\mathbf{1a}_2\cdot\mathbf{2b}$

X-ray quality, yellow single crystals of $\mathbf{1a}_2\cdot\mathbf{2b}$ were grown by vapor diffusion of pentane into an acetonitrile solution of **2b** with excess **1a**. The crystal structure of $\mathbf{1a}_2\cdot\mathbf{2b}$ (Fig. 6) is very similar to that of $\mathbf{1a}_2\cdot\mathbf{2a}$ in terms of interactions, including hydrogen bonding and face-to-face π-stacking between the bispyridinium guest and the cryptand hosts.

2.7. X-ray analysis of [3]pseudorotaxane $\mathbf{1b}_2\cdot\mathbf{2b}$

X-ray quality, yellow single crystals of $\mathbf{1b}_2\cdot\mathbf{2b}$ were grown by vapor diffusion of pentane into an acetone solution of **2b** with excess **1b**. The interactions between the hosts and the guest in the crystal structure of $\mathbf{1b}_2\cdot\mathbf{2b}$ (Fig. 7) are very similar to those in crystal structures of $\mathbf{1a}_2\cdot\mathbf{2b}$ and $\mathbf{1a}_2\cdot\mathbf{2a}$ because all of them include hydrogen bonding and face-to-face π-stacking between the bispyridinium guest and the cryptand hosts. However, this complex has some unique characteristics, which were not observed in $\mathbf{1a}_2\cdot\mathbf{2b}$ and $\mathbf{1a}_2\cdot\mathbf{2a}$. Firstly, both ends of bispyridinium guest **2b** are threaded unsymmetrically into the cavity of the 32-crown-10 part of the cryptand host in $\mathbf{1b}_2\cdot\mathbf{2b}$ (Fig. 7). This is similar to the complex based on cryptand host **1b** and paraquat guest.[4e] However, both ends of the bispyridinium are nearly symmetrically located in $\mathbf{1a}_2\cdot\mathbf{2b}$ and $\mathbf{1a}_2\cdot\mathbf{2a}$ (Figs. 5 and 6). Secondly, no hydrogen-bonding water bridges are observed between the cryptand host and bispyridinium guest in $\mathbf{1b}_2\cdot\mathbf{2b}$ (Fig. 7), while there are hydrogen-bonding water bridges at each end of the [3]pseudorotaxane between the cryptand host and bispyridinium guest in $\mathbf{1a}_2\cdot\mathbf{2b}$ and $\mathbf{1a}_2\cdot\mathbf{2a}$ (Figs. 5 and 6).

3. Conclusions

In summary, [3]pseudorotaxanes were successfully prepared by self-assembly between two cryptand hosts and two bispyridinium guests based on the cryptand/monopyridinium salt recognition motif as confirmed by proton NMR characterization, electrospray ionization mass spectrometry, and X-ray analysis. The formation of these cryptand/monopyridinium [3]pseudorotaxanes was mainly driven by hydrogen bonding, face-to-face π-stacking interactions, and charge transfer interactions. Currently we are preparing mechanically interlocked cryptand/monopyridinium [3]rotaxanes by introducing appropriate stoppers at the two ends of bispyridinium salts. We will also make bispyridinium guests with different spacers in order to learn how close the two pyridinium binding groups must be to influence each other.

4. Experimental section

4.1. General syntheses of bispyridinium salts 2

Compound **2a**: to a 50 mL three-necked round bottomed flask equipped with a magnetic stirrer and a condenser were added 1,4-di(bromomethyl)benzene (1.32 g, 5.00 mmol) and 10 mL acetonitrile. To this solution was added a solution of ethyl isonicotinate (15.1 g, 100 mmol) in 10 mL acetonitrile and the mixture was stirred at reflux for 48 h. The reaction mixture was cooled to room temperature and the precipitate was filtered. The solid was boiled in $CHCl_3$ and filtered. This solid was dissolved in a minimum volume of deionized water. To this solution was added NH_4PF_6 until no further precipitation was observed. The precipitate was filtered and recrystallized from deionized water three times to afford **2a** as white crystals, 3.06 g (88%), mp 236.8–238.1 °C. ^{1}H NMR (400 MHz, CD_3COCD_3, 22 °C): δ 9.50 (d, J=6.8 Hz, 4H), 8.73 (d, J=6.8 Hz, 4H), 7.79 (s, 4H), 6.29 (s, 4H), 4.54 (q, J=7.2 Hz, 4H), 1.44 (t, J=7.2 Hz, 6H). Elemental analysis calcd for $C_{24}H_{26}O_4N_2P_2F_{12}$: C, 41.37; H, 3.76; N, 4.02. Found: C, 41.51; H, 3.74; N, 4.13.

Compound **2b**: prepared in a similar way as **2a**, was obtained also as white crystals (85%), mp 179.8–180.8 °C. ^{1}H NMR (400 MHz, CD_3COCD_3, 22 °C): δ 9.43 (d, J=6.8 Hz, 4H), 8.71 (d, J=6.8 Hz, 4H), 5.03 (t, J=7.7 Hz, 4H), 4.55 (q, J=7.2 Hz, 4H), 2.29 (m, 4H), 1.66 (m, 4H), 1.45 (t, J=7.2 Hz, 6H). LRFABMS (matrix, NBA) m/z 531.7 $[M-PF_6]^+$, 386.6 $[M-2PF_6]^+$. HRFABMS (matrix, NBA/PEG) m/z calcd for $C_{22}H_{30}O_4N_2PF_6$, 531.1847 $[M-PF_6]^+$, found 531.1846, error 0.2 ppm.

Acknowledgements

This work was supported by the National Science Foundation (DMR0097126) and the Petroleum Research Fund (40223-AC7). We also thank the National Science Foundation for funding the purchase of the Oxford Diffraction Xcalibur2 diffractometer (CHE-0131128). F.H. thanks the National Natural Science Foundation of China (20604020) and Zhejiang Province (2006R10003) for financial support.

Supplementary data

Electrospray ionization mass spectra of solutions of **1a** and **2**. Supplementary data associated with this article can be found in the online version at doi:10.1016/j.tet.2007.01.029.

References and notes

1. (a) Reviews on threaded structures: Gong, C.; Gibson, H. W. *Curr. Opin. Solid State Mater. Sci.* **1997**, *2*, 647–652; Raymo, F. M.; Stoddart, J. F. *Chem. Rev.* **1999**, *99*, 1643–1663; *Molecular Catenanes, Rotaxanes and Knots*; Sauvage, J.-P., Dietrich-Buchecker, C. O., Eds.; Wiley-VCH: Weinheim, 1999; Mahan, E.; Gibson, H. W. *Cyclic Polymers*, 2nd ed.; Semlyen, J. A., Ed.; Kluwer: Dordrecht, 2000; pp 415–560; Hubin, T. J.; Busch, D. H. *Coord. Chem. Rev.* **2000**, *200–202*, 5–52; Pease, A. R.; Jeppesen, J. O.; Stoddart, J. F.; Luo, Y.;

Collier, C. P.; Heath, J. R. *Acc. Chem. Res.* **2001**, *34*, 433–444; Ballardini, R.; Balzani, V.; Credi, A.; Gandolfi, M. T.; Venturi, M. *Acc. Chem. Res.* **2001**, *34*, 445–455; Harada, A. *Acc. Chem. Res.* **2001**, *34*, 456–464; Panova, I. G.; Topchieva, I. N. *Russ. Chem. Rev.* **2001**, *70*, 23–44; Kim, K. *Chem. Soc. Rev.* **2002**, *31*, 96–107; Carlucci, L.; Ciani, G.; Proserpio, D. M. *Coord. Chem. Rev.* **2003**, *246*, 247–289; Huang, F.; Gibson, H. W. *Prog. Polym. Sci.* **2005**, *30*, 982–1018; (b) Recent publications on threaded structures: Leigh, D. A.; Wong, J. K. Y.; Dehez, F.; Zerbetto, F. *Nature* **2003**, *424*, 174–179; Huang, F.; Zakharov, L. N.; Rheingold, A. L.; Jones, J. W.; Gibson, H. W. *Chem. Commun.* **2003**, 2122–2123; Schalley, C. A.; Reckien, W.; Peyerimhoff, S.; Baytekin, B.; Vögtle, F. *Chem.—Eur. J.* **2004**, *10*, 4777–4789; Hernández, J. V.; Kay, E. R.; Leigh, D. A. *Science* **2004**, *306*, 1532–1537; Huang, F.; Gibson, H. W. *J. Am. Chem. Soc.* **2004**, *126*, 14738–14739; Huang, F.; Gibson, H. W. *Chem. Commun.* **2005**, 1696–1698; Qu, D.-H.; Wang, Q.-C.; He, T. *Angew. Chem., Int. Ed.* **2005**, *44*, 5296–5299.

2. Allwood, B. L.; Spencer, N.; Shahriari-Zavareh, H.; Stoddart, J. F.; Williams, D. J. *J. Chem. Soc., Chem. Commun.* **1987**, 1064–1066.
3. Zhao, X.; Jiang, X.-K.; Shi, M.; Yu, Y.-H.; Xia, W.; Li, Z.-T. *J. Org. Chem.* **2001**, *66*, 7035–7043; Chen, L.; Zhao, X.; Chen, Y.; Zhao, C.-X.; Jiang, X.-K.; Li, Z.-T. *J. Org. Chem.* **2003**, *68*, 2704–2712; Huang, F.; Fronczek, F. R.; Gibson, H. W. *Chem. Commun.* **2003**, 1480–1481; Huang, F.; Jones, J. W.; Slebodnick, C.; Gibson, H. W. *J. Am. Chem. Soc.* **2003**, *125*, 14458–14464; Huang, F.; Guzei, I. A.; Jones, J. W.; Gibson, H. W. *Chem. Commun.* **2005**, 1693–1695.
4. (a) Bryant, W. S.; Jones, J. W.; Mason, P. E.; Guzei, I. A.; Rheingold, A. L.; Nagvekar, D. S.; Gibson, H. W. *Org. Lett.* **1999**, *1*, 1001–1004; (b) Huang, F.; Fronczek, F. R.; Gibson, H. W. *J. Am. Chem. Soc.* **2003**, *125*, 9272–9273; (c) Huang, F.; Gibson, H. W.; Bryant, W. S.; Nagvekar, D. S.; Fronczek, F. R. *J. Am. Chem. Soc.* **2003**, *125*, 9367–9371; (d) Huang, F.; Zhou, L.; Jones, J. W.; Gibson, H. W.; Ashraf-Khorassani, M. *Chem. Commun.* **2004**, 2670–2671; (e) Huang, F.; Switek, K. A.; Zakharov, L. N.; Fronczek, F. R.; Slebodnick, C.; Lam, M.; Golen, J. A.; Bryant, W. S.; Mason, P.; Rheingold, A. L.; Ashraf-Khorassani, M.; Gibson, H. W. *J. Org. Chem.* **2005**, *70*, 3231–3241; (f) Huang, F.; Switek, K. A.; Gibson, H. W. *Chem. Commun.* **2005**, 3655–3657.
5. Huang, F.; Zakharov, L. N.; Rheingold, A. L.; Ashraf-Khorassani, M.; Gibson, H. W. *J. Org. Chem.* **2005**, *70*, 809–813; Zong, Q.-S.; Chen, C.-F. *Org. Lett.* **2006**, *8*, 211–214; Lin, C.-F.; Liu, Y.-H.; Lai, C.-C.; Peng, S.-M.; Chiu, S.-H. *Chem.—Eur. J.* **2006**, *12*, 4594–4599; Lin, C.-F.; Liu, Y.-H.; Lai, C.-C.; Peng, S.-M.; Chiu, S.-H. *Angew. Chem., Int. Ed.* **2006**, *45*, 3176–3181.
6. Han, T.; Chen, C.-F. *Org. Lett.* **2006**, *8*, 1069–1072.
7. Curiel, D.; Beer, P. D.; Paul, R. L.; Cowley, A.; Sambrook, M. R.; Szemes, F. *Chem. Commun.* **2004**, 1162–1163; Sambrook, M. R.; Beer, P. D.; Wisner, J. A.; Paul, R. L.; Cowley, A. R. *J. Am. Chem. Soc.* **2004**, *126*, 15364–15365.
8. (a) Huang, F.; Slebodnick, C.; Ratliff, A.; Gibson, H. W. *Tetrahedron Lett.* **2005**, *46*, 6019–6022; (b) Huang, F.; Slebodnick, C.; Rheingold, A. L.; Switek, K. A.; Gibson, H. W. *Tetrahedron* **2005**, *61*, 10242–10253.
9. Recent publications: (a) Yamada, D. S.; Misono, T.; Tsuzuki, S. *J. Am. Chem. Soc.* **2004**, *126*, 9682–9872; (b) Rashkin, M. J.; Hughes, R. M.; Calloway, N. T.; Waters, M. L. *J. Am. Chem. Soc.* **2004**, *126*, 13320–13325; (c) Zhao, D.; Fei, Z.; Geldbach, T. J.; Scopelliti, R.; Dyson, P. J. *J. Am. Chem. Soc.* **2004**, *126*, 15876–15882; (d) Pittelkow, M.; Christensen, J. B.; Meijer, E. W. *J. Polym. Sci. Polym. Chem.* **2004**, *42*, 3792–3799; (e) Vasilev, A.; Deligeorgiev, T.; Gadjev, N.; Drexhage, K.-H. *Dyes Pigments* **2005**, *66*, 135–142; (f) Ilies, M. A.; Johnson, B. H.; Makori, F.; Miller, A.; Seitz, W. A.; Thompson, E. B.; Balaban, A. T. *Arch. Biochem. Biophys.* **2005**, *435*, 217–226; (g) Tsuji, K.; Nishimura, N.; Duan, X.-M.; Okada, S.; Oikawa, H.; Matsuda, H.; Nakanishi, H. *Bull. Chem. Soc. Jpn.* **2005**, *78*, 180–186; (h) Colilla, M.; Darder, M.; Aranda, P.; Ruiz-Hitzky, E. *Chem. Mater.* **2005**, *17*, 708–715.
10. Cheng, P.-N.; Lin, C.-F.; Liu, Y.-H.; Lai, C.-C.; Peng, S.-M.; Chiu, S.-H. *Org. Lett.* **2006**, *8*, 435–438.
11. Olenyuk, B.; Whiteford, J. A.; Fechtenkötter, A.; Stang, P. J. *Nature* **1999**, *398*, 796–799; Hubbard, A. L.; Davidson, G. J. E.; Patel, R. H.; Wisner, J. A.; Loeb, S. J. *Chem. Commun.* **2004**, 138–139 and references therein; Qu, D.-H.; Wang, Q.-C.; Ma, X.; Tian, H. *Chem.—Eur. J.* **2005**, *11*, 5929–5937.
12. Marshall, A. G. *Biophysical Chemistry*; Wiley: New York, NY, 1978; pp 70–77; Freifelder, D. M. *Physical Biochemistry*; W.H. Freeman: New York, NY, 1982; pp 659–660; Connors, K. A. *Binding Constants*; Wiley: New York, NY, 1987; pp 78–86.
13. Tsukube, H.; Furuta, H.; Odani, A.; Takeda, Y.; Kudo, Y.; Inoue, Y.; Liu, Y.; Sakamoto, H.; Kimura, K. *Comprehensive Supramolecular Chemistry*; Atwood, J. L., Davies, J. E. D., MacNicol, D. D., Vogtle, F., Lehn, J.-M., Eds.; Elsevier: New York, NY, 1996; Vol. 8, p 425.
14. Δ_0, the difference in δ values for H_7 of **2a** in the uncomplexed and fully complexed species, was determined as the *y*-intercept of a plot of $\Delta=\delta-\delta_u$ versus $1/[\mathbf{1a}]_0$ in the high initial concentration range of **1a**; $\Delta_0=0.238$ ppm. Then $p=\Delta/\Delta_0$; $\Delta=$ observed chemical shift change relative to uncomplexed species.
15. Other examples of statistical complexation: Gibson, H. W.; Yamaguchi, N.; Hamilton, L.; Jones, J. W. *J. Am. Chem. Soc.* **2002**, *124*, 4653–4665; Huang, F.; Nagvekar, D. S.; Slebodnick, C.; Gibson, H. W. *J. Am. Chem. Soc.* **2005**, *127*, 484–485.
16. $K_1=[\mathbf{1a}\cdot\mathbf{2a}]/\{[\mathbf{1a}][\mathbf{2a}]\}$ and $K_2=[\mathbf{1a}_2\cdot\mathbf{2a}]/\{[\mathbf{1a}\cdot\mathbf{2a}][\mathbf{1a}]\}$. $K_{av}=(K_1+K_2)/2$. The value of K_{av} is equal to the average of the *y*-intercept (274 M^{-1}) and the absolute slope (288 M^{-1}) of the best fit line shown in Figure 4. Since $K_1/K_2=4:1$ for statistical systems,[12] K_1 and K_2 were calculated to be 112 and 448 M^{-1}.
17. Crystal data of $\mathbf{1a}_2\cdot\mathbf{2a}$: plate, yellow, $0.38\times0.23\times0.06$ mm, $C_{104}H_{150}O_{36}N_6P_2F_{12}$, FW 2350.24, triclinic, space group *P*-1, $a=10.5597(13)$, $b=16.0015(16)$, $c=18.397(2)$ Å; $\alpha=105.583(9)^\circ$, $\beta=105.919(10)^\circ$, $\gamma=91.528(9)^\circ$; $V=2862.6(6)$ Å^3, $Z=1$, $D_c=1.363$ g cm^{-3}, $T=100$ K, $\mu=1.40$ cm^{-1}, 13,273 measured reflections, 10,109 independent reflections, 802 parameters, $F(000)=1242$, $R_{int}=0.0250$, $R_1=0.0519$, $wR_2=0.1247$ [$I>2\sigma(I)$], maximum residual density 1.231 eÅ^{-3}, and GooF(F^2)=1.014. Crystal data of $\mathbf{1a}_2\cdot\mathbf{2b}$: plate, yellow, $0.33\times0.20\times0.09$ mm, $C_{47}H_{71}O_{18}N_1P_1F_6$, FW 1083.02, triclinic, space group *P*-1, $a=10.2668(10)$, $b=14.8351(16)$, $c=19.322(2)$ Å; $\alpha=97.430(9)^\circ$, $\beta=101.347(9)^\circ$, $\gamma=95.682(9)^\circ$; $V=2837.6(5)$ Å^3, $Z=2$, $D_c=1.268$ g cm^{-3}, $T=100$ K, $\mu=1.35$ cm^{-1}, 13,982 measured reflections, 10,042 independent reflections, 672 parameters, $F(000)=1146$, $R_{int}=0.0459$, $R_1=0.0612$, $wR_2=0.1617$ [$I>2\sigma(I)$], maximum residual density 0.0601 eÅ^{-3}, and

GooF(F^2)=1.026. Crystal data of $\mathbf{1b}_2\cdot\mathbf{2b}$: prism, pale yellow, 0.15×0.20×0.40 mm, $C_{53.10}H_{73.20}O_{16.70}N_1P_1F_6$, FW 1137.70, triclinic, space group *P*-1, *a*=11.1022(18), *b*=12.887(2), *c*=21.249(4) Å; α=88.214(16)°, β=82.710(15)°, γ=70.338(16)°; *V*=2839.6(9) Å^3, *Z*=2, D_c=1.331 g cm^{-3}, *T*=100 K, μ=1.36 cm^{-1}, 21,390 measured reflections, 16,475 independent reflections, 716 parameters, *F*(000)=1203, R_{int}=0.0245, R_1=0.0560, wR_2=0.1408 [$I>2\sigma(I)$], maximum residual density 0.813 eÅ^{-3}, and GooF(F^2)=0.948. These structures were solved by SHELXS-97[18] and refined by SHELXL-97.[19] Crystallographic data (excluding structure factors) for the structures in this paper have been deposited with the Cambridge Crystallographic Data Center as supplementary publication numbers CCDC 259498, 259499, and 619679. Copies of the data can be obtained, free of charge, on application to CCDC, 12 Union Road, Cambridge CB2 1EZ, UK [fax: +144 (0)1223 336033 or e-mail: deposit@ccdc.cam.ac.uk].

18. Sheldrick, G. M. *SHELXS-97: Program for the Solution of Crystal Structures*; University of Göttingen: Göttingen, Germany, 1990.
19. Sheldrick, G. M. *SHELXL-97: Program for the Refinement of Crystal Structures*; University of Göttingen: Göttingen, Germany, 1997.
20. The benzyl group is an electron-releasing group[21] so it can reduce the positive charge density on the pyridinium rings of monopyridinium salt **3** and bispyridinium salt **2a**. However, two pyridinium rings share one xylyl group in bispyridinium salt **2a** so this effect is weaker in **2a** than in **3**. This makes the positive charge density on the pyridinium rings of bispyridinium salt **2a** higher than that of monopyridinium salt **3**.
21. Hansch, C.; Leo, A.; Taft, R. W. *Chem. Rev.* **1991**, *91*, 165–195.